Aluminum as a pressure-transmitting medium cum pressure standard for x-ray diffraction experiments to 200 GPa with diamond anvil cells

Anil K. Singh[a)]
Materials Science Division, National Aerospace Laboratories, Bangalore 560 017, India

Hanns-Peter Liermann
HPCAT, Advanced Photon Source, Argonne National Laboratory, Argonne, Illinois 60439

Yuichi Akahama and Haruki Kawamura
Graduate School of Materials, University of Hyogo, 3-2-1, Kouto, Kamigohri, Hyogo 678-1297, Japan

(Received 16 February 2007; accepted 17 March 2007; published online 27 June 2007)

The compressive strength of 99.999% pure aluminum as a function of pressure to 215 GPa has been determined from the linewidth analysis of high-pressure x-ray diffraction patterns recorded with beveled-diamond anvil cell. The strength is found to increase linearly from 0.3(1) GPa at zero pressure to 5.0(2) GPa at 200 GPa. The data to 55 GPa with flat anvil diamond cell suggest that the strength of 99.999% pure aluminum increases from 0.21(8) GPa at zero pressure to 1.1(1) GPa at 55 GPa and the extrapolated strength at 200 GPa is 3.3(4). Significantly larger strength obtained with beveled-diamond anvil cell most likely arises due to larger radial stress gradients than in the case of flat anvils. The strength of aluminum is compared with those of argon to 50 GPa and of helium to 70 GPa. The use of face-centered cubic phase of aluminum in the dual role of a pressure standard and solid pressure-transmitting medium to 200 GPa is discussed. © *2007 American Institute of Physics*. [DOI: 10.1063/1.2734868]

I. INTRODUCTION

Solid sample compressed in a diamond anvil cell (DAC) develops nonhydrostatic stresses.[1] For an unambiguous interpretation of the high-pressure data and its comparison with the theoretical predictions, it is desirable to carry out the measurements under hydrostatic pressure. The pressure on the sample can be rendered hydrostatic by confining the sample and a fluid pressure-transmitting medium (PTM) in a metal gasket. Ideally, PTM should remain a fluid and fully surround the sample to the highest pressure of the experiment. However, most fluids exhibit increase in viscosity and ultimately freeze as the pressure is increased. This results in a gradual increase of nonhydrostatic stresses on the sample. A fluid PTM is much more compressible than the solid sample. This can result in the sample bridging the anvils at pressures much lower than the pressure range where appreciable PTM-viscosity increase or freezing occurs. With the limited volume of the high-pressure chamber of the DAC, the sample bridging the anvils can be postponed to higher pressures by reducing the sample-volume to PTM-volume ratio. However, the sample volume cannot be reduced below a limit if reasonable signal-to-background ratio is to be obtained. Helium, the best-known PTM, retains fluidlike flow property to much higher pressures than any other fluid. The highest hydrostatic pressure that can be achieved with He as a PTM has been examined by many investigators. Bell and Mao[2] measured the pressures at different locations in the pressure chamber filled with He using ruby chips, and reported a maximum pressure difference less than 0.6% at 60 GPa. Based on the rocking curve of 440 reflection of diamond single crystal immersed in He, Alexandrov *et al.* detected the onset of nonhydrostatic stresses above 35 GPa.[3] Li and Ahsbahs observed no broadening of diffraction peaks of pyrope in He as PTM up to 33 GPa.[4] Zha *et al.* reported high-quality Brillouin scattering data on MgO up to 55 GPa.[5] Takemura examined the diffraction linewidths of CeO_2, high-pressure phase of ZnO, and Au to establish the upper hydrostatic-pressure limit of He PTM and found no evidence of nonhydrostaticity up to 77 GPa.[6] Singh and Takemura used the lattice strain theory[1] to analyze the powder diffraction data on Nb taken with He as PTM and detected the presence of nonhydrostatic stresses at pressures as low as 20 GPa.[7] Dewaele *et al.* studied the compression behavior of cubic metals above 94 GPa with He as a PTM ensuring that sample did not bridge the anvils by maintaining the sample thickness less than the gasket thickness in the entire pressure range of the experiments.[8] These authors did not find any evidence of nonhydrostatic compression up to the highest pressures (~150 GPa) in their experiments. Obviously, the upper limit of hydrostatic pressure achieved in an experiment depends on the details of the cell loading, the elastic-plastic properties of the solid sample, and the property measured to detect the onset of nonhydrostatic pressure. He-PTM under high pressure is known to diffuse in diamond anvils, leading to breakage of the anvils and thus posing some practical problems.[9] Further, loading of He in the cell requires a special setup.

The use of a soft solid, a low shear strength material, as a PTM has the advantages that the difference between the compressibility of sample and that of the PTM is greatly reduced and, thereby, the problem of sample bridging the anvils is less serious. Further, containing a solid in the gasket

[a)]Author to whom correspondence should be addressed; Electronic mail: aksingh@css.nal.res.in

without leakage is considerably simpler than sealing fluid PTM. In the past, several soft solids have been used as PTM. For example, Singh and Kennedy measured pressure-volume relations of MgO, Si, and $ZrSiO_4$ with epoxy as the PTM.[10] In particular, the compressibility data of $ZrSiO_4$ determined by Singh and Kennedy were found to agree very well with the result of a more recent single-crystal x-ray diffraction study carried out with methanol-ethanol mixture as the PTM.[11] Bassett *et al.* used sodium chloride as the PTM to measure the equation of state of SiC,[12] and Hanfland *et al.* reported the equation of state of Ta measured with Na as the PTM.[13]

In addition to low shear strength, the solid PTM should have low absorption for the wavelength (~0.03–0.06 nm) of x rays used in diffraction work with a DAC. The low absorption will permit large PTM volume to sample volume ratio, a requirement for efficient pressure transmission. The solid PTMs used so far are mostly crystalline and the diffraction lines from the PTM often interfere with the diffraction pattern from the sample. If the pressure is measured by mixing the sample with another crystalline solid (pressure standard or marker) of known equation of state, then one has to deal with three sets of diffraction patterns recorded together. No doubt, the peaks can be separated using suitable software, but this is not without the loss of precision in the determination of the diffraction-line positions and widths. In this respect, the use of a PTM with well-characterized equation of state has a definite advantage, as it can be used in the dual role of a PTM and pressure standard. High-purity Al appears to have all the properties required for a PTM and pressure standard. The yield stress of high-purity annealed Al at ambient condition is 20 MPa.[14] With atomic number 13, the absorption factors of Al for range of x-ray wavelengths used in experiments with a DAC are low and the equation of state (EOS) is well studied.[8,15–24] Though Liermann *et al.* studied transition metal carbides under high pressure using high-purity aluminum both as a PTM and pressure standard,[25,26] the strength of Al at high pressures remained to be examined. This aspect is important for establishing Al as a PTM because Al will undergo severe deformation during the initial compression in a DAC, and pure Al is known to exhibit significant strain-hardening effect that would result in the increase of compressive strength.[14]

In this article we analyze the linewidths of high-pressure x-ray diffraction patterns taken with diamond anvil cell (DAC) to derive the compressive strength of Al as a function of pressure to 215 GPa, a pressure range over which the face-centered cubic phase is stable.[24] The strength data on Al are compared with the recent estimates of strengths under pressure of argon[27] and helium.[28]

II. EXPERIMENTAL DETAILS

The diffraction data from two sets of experiments were used in the present study. The DAC (300 μm flat anvil faces) was used in the first set of experiments to compress the sample. The Al sample (sample A) was 99.999% pure from Goodfellow Corp. Pa. (major impurities: Ca–3 ppm, Cr–2, Cu–<1, Fe–2, Mg–<1, Si–1, Ag–<1). The sample was contained in a stainless-steel gasket with indentation depth 32 μm and central hole of 90 μm diameter. No pressure-transmitting medium was used to maximize the nonhydrostatic stress component. The diffraction experiments were carried out using the Insertion Device Beamline of the HP-CAT at the Advanced Photon Source (APS), Argonne National Laboratory, Chicago. The incident beam of wavelength 0.036 81 nm was collimated to 10×10 μm^2 size. The pressure was increased in steps of ~5 GPa and the diffraction patterns were recorded online at each pressure on an image plate. The pressure in each run was obtained from the experimental EOS (Ref. 7) and the measured volume compression of Al. The maximum pressure reached in these experiments was 55 GPa. The second set of data used in this study was obtained in an earlier study.[24] These experiments were conducted with beveled-diamond anvils of two different face diameters (35 and 50 μm) and the sample (sample B), also 99.999% pure, was contained in rhenium gaskets. The incident beam of wavelength 0.049 57 nm was collimated to 10 μm diameter. The pressures in excess of 300 GPa, measured on platinum pressure scale,[29] could be reached. The data only to 215 GPa were used in this analysis, as the fcc phase transforms to hcp at higher pressure. The four-parameter pseudo-Voigt function was fitted to the diffraction peaks and the peak position and full width at half maximum (FWHM) were determined.

III. METHOD OF DATA ANALYSIS

The solid sample between the diamond anvils undergoes considerable deformation in the initial stages of compression. Complex stresses are established when the flow ceases and equilibrium is reached. Generally, the stress state is considered as a superposition of macro- and microstresses. The macrostresses produce strains that cause the diffraction lines to shift, and microstresses result in the broadening of lines. The analysis of the line shift gives valuable information on the compressive strength and elasticity of the solid sample.[1] The strength of the solid sample as a function of pressure also has been estimated from the linewidth analysis in a number of studies.[30–37] Underlying these analyses is the model for microstresses proposed by Stokes and Wilson[38] that assumes that the stresses in cold-worked metals vary between zero and the maximum stress p_{max} with equal probability. The maximum stress p_{max} is a measure of the compressive strength of the sample material.[39] The model of Stokes and Wilson has to be modified for the sample compressed in a DAC by noting that the microstresses vary between $p(\min)$ and $p(\max)$, the pressure on the sample being $[p(\min)+p(\max)]/2$. Thus, the difference between $p(\max)$ and $p(\min)$ is p_{max} of Stokes and Wilson.[38] Noting that the dependence of linewidth on the grain size varies as $1/\cos\theta$ and on the strain as $\tan\theta$, the following relation can be obtained:[40]

$$(2w_{hkl}\cos\theta_{hkl})^2 = (\lambda/D)^2 + \eta_{hkl}^2 \sin^2\theta_{hkl}. \quad (1)$$

Here, $2w_{hkl}$, θ_{hkl}, λ, D, and η_{hkl} are the linewidth, Bragg angle, x-ray wavelength, grain size (assumed to be *hkl*-independent), and microstrain, respectively. Equation (1)

is strictly valid for the Gaussian profiles and is appropriate for analyzing high-pressure diffraction patterns wherein the major source of broadening is the microstrain. The strain η_{hkl} in terms of the single-crystal Young's modulus $E(hkl)$ is given by the following relation:[38]

$$\eta_{hkl} = 4p_{\max}/E(hkl). \quad (2)$$

By combining Eqs. (1) and (2), we get

$$(2w_{hkl}\cos\theta_{hkl})^2 = (\lambda/D)^2 + [4p_{\max}/E(hkl)]^2\sin^2\theta_{hkl}. \quad (3)$$

The $(2w_{hkl}\cos\theta_{hkl})^2$ vs $\sin^2\theta_{hkl}/E^2(hkl)$ plots represent a straight line; D and $p_{\max}$ can be determined from such plots. To a good approximation, the $(2w_{hkl}\cos\theta_{hkl})^2$ vs $\sin^2\theta_{hkl}$ plot also represents a straight line. Equation (1) can be used directly when the single-crystal data are not available to compute $E(hkl)$ required in Eq. (3). The strain determined from the slope of the $(2w_{hkl}\cos\theta_{hkl})^2$ vs $\sin^2\theta_{hkl}$ is the average strain $\langle\eta\rangle$, and $p_{\max}$ is given by the relation

$$\langle\eta\rangle = 4p_{\max}/E. \quad (4)$$

Here, E is the Young's modulus of the polycrystalline aggregate.

In several high-pressure studies,[30–37] the parameter $2p_{\max}$ has been taken as a measure of the compressive strength. The macrostress at the center of the sample is axially symmetric about the load axis of the DAC, and the difference between the axial and radial stress components t is also a measure of the compressive strength of the sample at a pressure that equals the mean normal stress.[1,41–43] The high-pressure x-ray studies on magnesium oxide,[34] gold,[36] and iron[37] show that t and $2p_{\max}$ are comparable in magnitude.

It may be noted that several other methods of analyzing the diffraction line profiles to derive grain size and microstrains can be found in the literature. These are the full line profile analysis,[44] single-peak methods,[45] and variance-based methods.[46] These methods are expected to give more reliable information on grain size and strain than simple treatment provided by Eq. (1) but require high-precision diffraction profile data as the input. The high-pressure data are vitiated to some extent by the presence of radial stress gradients in the sample; therefore, the present study uses Eq. (1) to analyze diffraction linewidths.

IV. GRAIN SIZE AND STRENGTH DATA

First, Eq. (1) was used to determine D and $\langle\eta\rangle$. Figure 1 shows typical $(2w\cos\theta)^2$ vs $\sin^2\theta$ plots for aluminum. Such plots were constructed for each run and straight lines fitted by the method of least-squares. The values of D and $\langle\eta\rangle$ at different pressures were obtained from the intercept and slope of the straight lines. The Young's modulus required in Eq. (4) was obtained by the relation

$$E = 9GK/(3K+G), \quad (5)$$

where K and G are the bulk and shear moduli of the aggregate, respectively. K as a function of pressure was obtained numerically from the 300 K isotherm[22] and G was computed from the Simon-type function,[47]

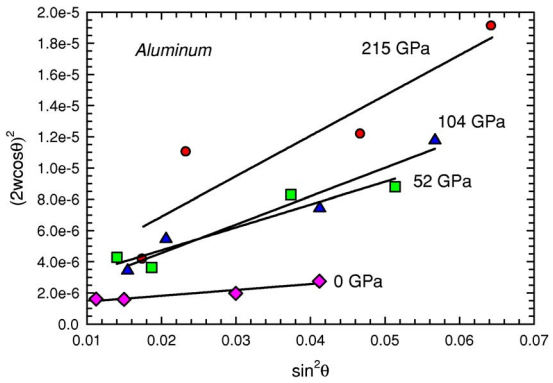

FIG. 1. (Color online) $(2w\cos\theta)^2$ vs $\sin^2\theta$ plots at different pressures.

$$G = 29.3(1 + P/12.9)^{0.70}. \quad (6)$$

This relation is expected to be valid to 1500 GPa.[47] The results of Eq. (6) and the commonly used Birch extrapolation formula[48] with 72.7, 29.3 GPa and 1.8 for the ambient pressure bulk modulus, shear modulus, and pressure derivative of shear modulus, respectively, begin to diverge with increasing pressure. At 200 GPa, Birch extrapolation formula gives ~13% higher shear modulus than Eq. (6). The errors in $2p_{\max}$ introduced by the uncertainty in the values of E at high pressures are much smaller than those due to the experimental errors.

Next, Eq. (3) was used to determine D and $2p_{\max}$. The $E(hkl)$ values were computed from the Birch extrapolation formula[48] using the single-crystal elasticity data obtained from ultrasonic experiments.[49] The strength determined by the two methods agreed very well, the maximum difference being 8% at the highest pressure. The grain sizes were also comparable. For sake of clarity, the results from the first method only are shown.

The initial grain sizes of both samples are >300 nm and remain practically unchanged with increasing pressure [Fig. 2]. The pressure dependence of the grain size observed earlier for gold[36] is not seen here. The initial grain size in the present case is large and consequently the intercept of the $(2w\cos\theta)^2$ vs $\sin^2\theta$ lines small. The precision in determination of the intercepts of the lines is not high enough to detect changes in the grain size induced by pressure. In the case of gold,[36] the initial grain sizes of the two samples were

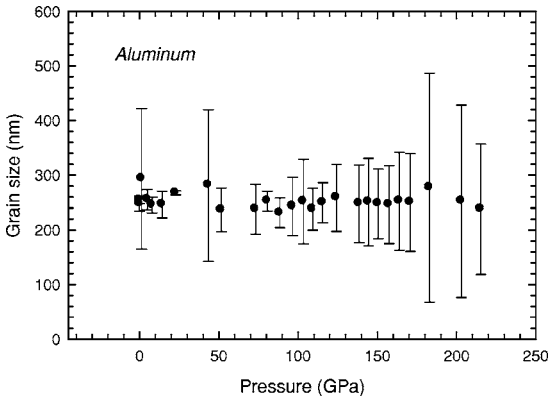

FIG. 2. Grain size as a function of pressure.

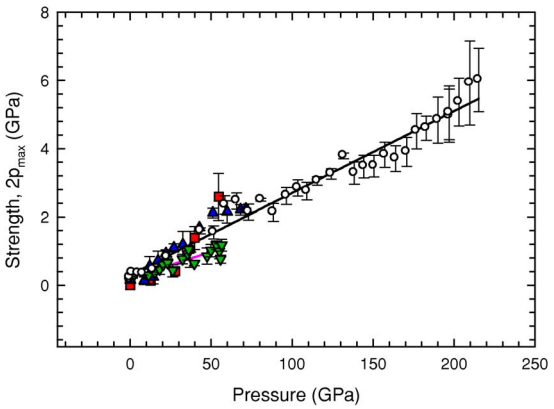

FIG. 3. (Color online) A comparison of the strengths of aluminum, argon, and helium at different pressures. Triangles down—Al sample A; unfilled circles—Al sample B; squares—argon; triangles up—helium.

120(15) nm and 33(3) nm. The intercepts of the $(2w\cos\theta)^2$ vs $\sin^2\theta$ lines were large, and pressure-induced changes in the grain size could be detected.

The strengths $(2p_{\max})$ determined from Eq. (4) at different pressures for samples A and B are shown in Fig. 3. The compressive yield strength for sample A showed a linear increase with pressure according to the relation

$$2p_{\max} = 0.21(\pm 0.08) + 0.0153(\pm 0.0022)P. \quad (7)$$

Sample B also exhibited a similar trend, given by

$$2p_{\max} = 0.3018(\pm 0.0956) + 0.0240(\pm 0.0007)P. \quad (8)$$

At all pressures, the strength of sample B is significantly higher than that of sample A. At 200 GPa, the strengths of sample A and sample B as calculated from Eqs. (7) and (8) are 3.3 and 5.1 GPa, respectively. As both samples were 99.999% pure, the sample purity is unlikely to be the factor causing this difference. Larger stress gradients in the experiments with the beveled anvils (sample B) may cause this difference. Therefore, the actual strength of high-purity Al is likely to be closer to that for sample A. For comparison, the strengths of argon[27] and helium,[7,28] both considered to be good pressure-transmitting media, are also given in Fig. 3. The strength of argon is small (<0.1 GPa) below 10 GPa and increases steeply with increasing pressure. Above 40 GPa pressure, the strength of argon exceeds that of aluminum. The strength of helium is small (<0.1 GPa) at pressures below 15 GPa and increases with increase in pressure so rapidly that at 50 GPa it becomes comparable to the strength of Al. It may be noted that the strength of He was estimated from the analysis of strains in Nb samples placed in He-PTM.[7,28] Care was taken to ensure that the sample did not bridge the anvils by keeping the initial sample thickness less than the gasket thickness at the highest pressure of the experiment. These estimates of the strength of He under pressure are much higher than those of Dewaele *et al.*, who did not find any evidence of nonhydrostatic stresses up to ~150 GPa in the powder samples of Pt, Cu, and Au.[8] This disagreement necessitates a reexamination of the strength of He under pressure.

V. EQUATION OF STATE OF AL

A. Measured EOS

Syassen and Holzapfel measured EOS of Al to 12 GPa using NaCl as the pressure standard with tungsten carbide anvils.[21] Green *et al.* used DAC to compress Al samples and measured the pressure-volume relation of Al up to 200 GPa using Pt pressure standard.[22] Akahama *et al.* used beveled-anvil DAC to measure the pressure-volume relation of Al to 333 GPa also using Pt pressure standard.[24] Since Pt scatters x rays much more strongly than Al, these experiments employed large Al-volume to Pt-volume ratio. In both experiments Al acted as the PTM. Dewaele *et al.* measured the pressure-volume relation up to 144 GPa using He as the PTM and ruby fluorescence technique for pressure measurements.[8] Nellis *et al.* combined the shock compression data and first-principles calculations to propose the 300 K isotherm of Al up to 1000 GPa.[23] No phase transition under pressure was detected in the shock compression experiments, whereas Akahama *et al.* reported a phase transition from face-centered cubic to hexagonal close-packed structure at 217±10 GPa.[24]

B. Compression data from Holzapfel EOS

The one-parameter equation of state,[50–54] based on the assumption that under very strong compression $(P\to\infty)$ all solids approach the Thomas-Fermi state, has a certain degree of predictive capability. The pressure-volume relation for the Thomas-Fermi state is given by[55]

$$P = 1003.6(Z/V)^{5/3}. \quad (9)$$

Here, Z and V are the atomic number and molar volume (cm^3/mol), and the pressure P is in GPa. Holzapfel[49,53] proposed the following EOS for compressions at finite pressures:

$$P = 3K_0(x^5 - x^4)\exp\left[\tfrac{3}{2}(K_0' - 3)(1 - 1/x)\right], \quad (10)$$

where $x=(\rho/\rho_0)^{1/3}=(V_0/V)^{1/3}$. K_0 and K_0' are the one-atmosphere isothermal bulk modulus and its pressure derivative, respectively. Equation (10) is the same as Eq. H02 of Schulte and Holzapfel.[53] Under very strong compression, i.e., $P\to\infty$ and $\rho\to\infty$ (or equivalently, $V\to 0$), Eq. (10) reduces to

$$P = 3K_0x^5\exp\left[\tfrac{3}{2}(K_0' - 3)\right]. \quad (11)$$

K_0' in Eq. (10) is fixed by assuming that any EOS approaches Eq. (9) under strong compression . On combining Eqs. (9) and (11), we get the following relation:

$$K_0\exp\left[\tfrac{3}{2}(K_0' - 3)\right] = 334.53(Z/V_0)^{5/3} = C. \quad (12)$$

Elimination of K_0' from Eq. (10) using Eq. (12) gives

$$P = 3K_0(x^5 - x^4)(C/K_0)^{(1-1/x)}. \quad (13)$$

Equation (13) requires only the bulk modulus at zero (ambient) pressure as the input to compute the pressure-volume data for a solid. Green *et al.* pointed out that the one-parameter EOS predicts compression data of Al that are in excellent agreement with the measured data.[22]

TABLE I. The bulk modulus and pressure derivative of Al from various studies.

K_0	K_0'	Equation type	Reference
72.7 (fixed)	4.30	Birch	21
72.7 (fixed)	4.14	Birch	22
72.7 (fixed)	4.83	Vinet	24
73 (fixed)	4.54	Vinet	8
75.8(2)	4.109(3)	Birch	23
72.7 (input)	4.32	One-parameter EOS	52
72.7	4.42	Ultrasonic	21 and 54

C. Comparison of the pressure-volume data

The K_0 and K_0' in various studies have been derived by the authors by fitting either the third-order Birch or Vinet EOS to the compression data. These values, along with the values derived from the ultrasonic-velocity measurements, are listed in Table I. For a comparison of the pressure-volume data from various studies, the data of Nellis *et al.*,[23] which are from 86–1018 GPa, were used as the reference. To obtain data in the range 0–86 GPa, both Birch and Vinet EOS were fitted. The Birch EOS was found to fit significantly better than the Vinet EOS. The K_0 and K_0' obtained from the fit of Birch EOS are given in Table I. Because of the limited precision and the pressure range over which measurements were made, the data from Syassen and Holzapfel[21] are not discussed further. The V/V_0 values in the pressure range 86–1018 GPa were those from Table I of Nellis *et al.*[23] Seven compression values were selected between 0.634 and 0.96 and the corresponding pressures calculated from the Birch EOS with the values of K_0 and K_0' listed in Table I. For these V/V_0 values, the pressures were computed using the K_0 and K_0' values with the EOS indicated in Table I. The pressures were computed for different V/V_0 values using Eq. (13) with 72.7 GPa and 528.29 for the values of K_0 and C, respectively. The pressures are compared in Fig. 4. Even though the highest pressures in the measurement by Green *et al.*[22] and Dewaele *et al.*[8] are to 200 and 144 GPa, respectively, the agreement is within ~5% up to ~500 GPa. The pressures derived from the measurements by Akahama *et al.*,[24] however, show much larger deviation (<10%) from the corresponding pressures from the measurements of Nellis *et al.*[23] With the deviation ≤2% in the pressure range 25–1018 GPa and <3% at lower pressures, the results of Eq. (13) show excellent agreement with the data of Nellis *et al.*[23] The overall agreement among the results of different investigators[8,22,23] is very good. While using Al as the pressure standard, the pressures can be conveniently calculated from Eq. (13) using the x-ray measured V/V_0.

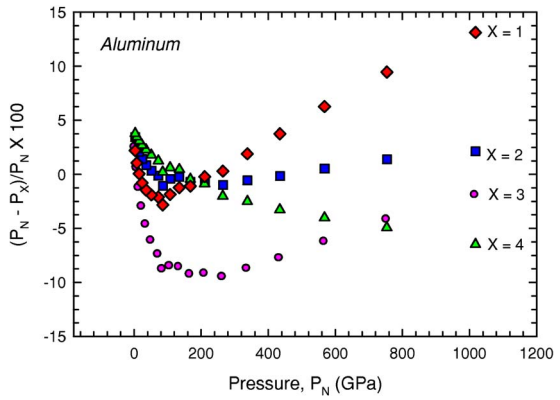

FIG. 4. (Color online) A comparison of the computed pressures from various equations of states of aluminum at different volume compressions. Pressure $P_1, X=1$, diamonds—Dewaele *et al.* (Ref. 9); $P_2, X=2$, squares—Holzapfel equation of state (Refs. 49–53); $P_3, X=3$, circles—Akahama *et al.* (Ref. 24); $P_4, X=4$, triangles—Green *et al.* (Ref. 22); P_N—Nellis *et al.* (Ref. 23).

VI. SUMMARY

With the low yield strength and absorption coefficient for x rays in the wavelength range used with diamond anvil cell, and well established equation of state, fcc-Al is ideally suited for the combined role of a solid pressure-transmitting medium and pressure standard, particularly in the study of samples with large compressive strength. A few studies made with fcc-Al as a pressure-transmitting medium and a pressure standard have yielded good results.

ACKNOWLEDGMENTS

The x-ray diffraction experiments to 55 GPa were carried out at HPCAT (Sector 16), Advanced Photon Source, ANL. Use was supported by DOE-BES (Contract No. W-31–109-ENG-38), DOE-NNSA (CDAC), NSF, DOD-TACOM, and W. M. Keck Foundation. The x-ray diffraction data to 215 GPa were obtained at SPring-8 under Proposals No. 2004A0541-ND2a-np and No. 2005B0190-ND2a-np approved by JASRI.

[1] A. K. Singh, J. Phys. Chem. Solids **65**, 1589 (2004).
[2] P. M. Bell and H. K. Mao, Carnegie Inst. Washington Publ. **80**, 404 (1981).
[3] L. V. Alexandrov, A. F. Gonchrov, A. N. Zosman, and S. M. Stishov, Sov. Phys. JETP **66**, 384 (1987).
[4] L. Zhang, H. Ahsbahs, and A. Kuteglu, Phys. Chem. Miner. **25**, 301 (1998).
[5] C. S. Zha, H. K. Mao, and R. J. Hemley, Proc. Natl. Acad. Sci. U.S.A. **97**, 13494 (2000).
[6] K. Takemura, J. Appl. Phys. **89**, 662 (2001).
[7] A. K. Singh and K. Takemura, J. Appl. Phys. **90**, 3269 (2001).
[8] A. Dewaele, P. Loubeyre, and M. Mezouar, Phys. Rev. B **70**, 094112 (2004).
[9] A. Dewaele, P. Loubeyre, R. André, and J. Härtwig, J. Appl. Phys. **99**, 104906 (2006).
[10] A. K. Singh and G. C. Kennedy, J. Appl. Phys. **48**, 3362 (1977).
[11] R. M. Hazen and L. W. Finger, Am. Mineral. **64**, 196 (1979).
[12] W. A. Bassett, M. S. Weathers, T. C. Wu, and T. Holmquist, J. Appl. Phys. **74**, 3824 (1993).
[13] M. Hanfland, K. Syassen, and J. Köhler, J. Appl. Phys. **91**, 4143 (2002).
[14] *Smithell's Metals Reference Book*, edited by E. A. Brandes (Butterworths, London, 1983), pp. 22–23.
[15] C. Friedli and N. W. Ashcroft, Phys. Rev. B **12**, 5552 (1975).
[16] P. K. Lam and M. L. Cohen, Phys. Rev. B **24**, 4224 (1981).
[17] J. A. Moriarty and A. K. McMahan, Phys. Rev. Lett. **48**, 809 (1982).
[18] A. K. McMahan and J. A. Moriarty, Phys. Rev. B **27**, 3235 (1983).
[19] P. K. Lam and M. L. Cohen, Phys. Rev. B **27**, 5986 (1983).
[20] J. C. Boettger and S. B. Trickey, Phys. Rev. B **53**, 3007 (1996).
[21] K. Syassen and W. B. Holzapfel, J. Appl. Phys. **49**, 4427 (1978).
[22] R. G. Greene, H. Luo, and A. L. Ruoff, Phys. Rev. Lett. **73**, 2075 (1994).
[23] W. J. Nellis, J. A. Moriarty, A. C. Mitchell, M. Ross, R. G. Dandrea, N. W. Ashcroft, N. C. Holmes, and G. R. Gathers, Phys. Rev. Lett. **60**, 1414 (1988).
[24] Y. Akahama, M. Nishimura, K. Kinoshita, and H. Kawamura, Phys. Rev. Lett. **96**, 045505 (2006).

[25]H. P. Liermann, A. K. Singh, B. Manoun, S. K. Saxena, V. B. Prakapenka, and G. Shen, Int. J. Refract. Met. Hard Mater. **22**, 129 (2004).
[26]H. P. Liermann, A. K. Singh, B. Manoun, S. K. Saxena, and C. S. Zha, Int. J. Refract. Met. Hard Mater. **23**, 109 (2005).
[27]H. K. Mao, J. Badro, J. Shu, R. J. Hemley, and A. K. Singh, J. Phys. Condens. Matter **18**, S963 (2006).
[28]K. Takemura and A. K. Singh, Phys. Rev. B **73**, 224119 (2006).
[29]N. C. Holmes, J. A. Moriarty, G. R. Gathers, and W. J. Nellis, J. Appl. Phys. **66**, 2962 (1989).
[30]A. K. Singh, K. Vijayan, H. Xia, Y. K. Vohra, and A. L. Ruoff, in *Recent Trends in High Pressure Research*, Proceedings of the 13th AIRAPT-International Conference on High Pressure Science and Technology, edited by A. K. Singh (Oxford IBH, New Delhi, 1992), pp. 782–785.
[31]D. J. Weidner, Y. Wang, and M. T. Vaughan, Science **266**, 419 (1994).
[32]J. Chen, T. Inoue, D. J. Weidner, Y. Wu, and M. T. Vaughan, Geophys. Res. Lett. **25**, 1103 (1998).
[33]J. Chen, D. J. Weidner, and M. T. Vaughan, Nature **419**, 824 (2002).
[34]A. K. Singh, H. P. Liermann, and S. K. Saxena, Solid State Commun. **132**, 795 (2004).
[35]J. Chen, N. Schmidt, J. Chen, L. Wang, D. Weidner, J. Zhang, and Y. Wang, J. Mater. Sci. Lett. **40**, 5763 (2005).
[36]A. K. Singh, H. P. Liermann, S. K. Saxena, H. K. Mao, and S. Usha Devi, J. Phys. Condens. Matter **18**, S969 (2006).
[37]A. K. Singh, A. Jain, H. P. Liermann, and S. K. Saxena, J. Phys. Chem. Solids **67**, 2197 (2006).
[38]A. R. Stokes and A. J. C. Wilson, Proc. Phys. Soc. Lond. **56**, 174 (1944).
[39]A. R. Stokes, K. J. Pascoe, and H. Lipson, Nature **151**, 137 (1943).
[40]J. I. Langford, J. Appl. Cryst. **4**, 164 (1971).
[41]A. K. Singh and G. C. Kennedy, J. Appl. Phys. **45**, 4686 (1974).
[42]A. L. Ruoff, J. Appl. Phys. **46**, 1389 (1975).
[43]A. K. Singh and G. C. Kennedy, J. Appl. Phys. **47**, 3337 (1976).
[44]B. E. Warren, *X-ray Diffraction* (Dover, New York, 1990).
[45]Th. H. de Keijser, J. I. Langford, E. J. Mittemeijer, and A. P. B. Vogels, J. Appl. Cryst. **15**, 308 (1982).
[46]F. Sànchez-Bajo and F. L. Cumbrera, J. Appl. Cryst. **30**, 427 (1997).
[47]L. Burakovsky and D. L. Preston, J. Phys. Chem. Solids **67**, 1930 (2006).
[48]F. Birch, J. Geophys. Res. **83**, 1257 (1978).
[49]J. F. Thomas, Phys. Rev. **175**, 955 (1968).
[50]W. B. Holzapfel, Europhys. Lett. **16**, 67 (1991).
[51]O. Schulte and W. B. Holzapfel, Phys. Rev. B **48**, 767 (1993).
[52]O. Schulte and W. B. Holzapfel, Phys. Rev. B **52**, 12636 (1995).
[53]O. Schulte and W. B. Holzapfel, Phys. Rev. B **53**, 569 (1996).
[54]W. B. Holzapfel, Rep. Prog. Phys. **59**, 29 (1996).
[55]N. N. Kalitkin and L. V. Kuz'mina, Dokl. Akad. Nauk **387**, 40 (2002); Dokl. Phys. **47**, 778 (2002).